



3-2019

Optimal Homotopy Asymptotic Solution for Thermal Radiation and Chemical Reaction Effects on Electrical MHD Jeffrey Fluid Flow Over a Stretching Sheet through Porous Media with Heat Source

Gossaye Aliy
Osmania University

Naikoti Kishan
Osmania University

Follow this and additional works at: <https://digitalcommons.pvamu.edu/aam>




Part of the [Fluid Dynamics Commons](#), and the [Partial Differential Equations Commons](#)

Recommended Citation

Aliy, Gossaye and Kishan, Naikoti (2019). Optimal Homotopy Asymptotic Solution for Thermal Radiation and Chemical Reaction Effects on Electrical MHD Jeffrey Fluid Flow Over a Stretching Sheet through Porous Media with Heat Source, *Applications and Applied Mathematics: An International Journal (AAM)*, Vol. 14, Iss. 4, Article 12.

Available at: <https://digitalcommons.pvamu.edu/aam/vol14/iss4/12>

This Article is brought to you for free and open access by Digital Commons @PVAMU. It has been accepted for inclusion in *Applications and Applied Mathematics: An International Journal (AAM)* by an authorized editor of Digital Commons @PVAMU. For more information, please contact hvkoshy@pvamu.edu.

	Available at http://pvamu.edu/aam Appl. Appl. Math. ISSN: 1932-9466 AAM Special Issue No. 4 (March 2019), pp. 150 - 175	Applications and Applied Mathematics: An International Journal (AAM)
---	--	---

Optimal Homotopy Asymptotic Solution for Thermal Radiation and Chemical Reaction Effects on Electrical MHD Jeffrey Fluid Flow Over a Stretching Sheet through Porous Media with Heat Source

*Gossaye Aliy and Naikoti Kishan

Department of Mathematics
Osmania University
Hyderabad, India

*Corresponding Author, gosyy610@gmail.com

Received: August 4, 2018; Accepted: October 28, 2018

Abstract

In this paper, the problem of thermal radiation and chemical reaction effects on electrical MHD Jeffrey fluid flow over a stretching surface through a porous medium with the heat source is presented. We obtained the approximate analytical solution of the nonlinear differential equations governing the problem using the Optimal Homotopy Asymptotic Method (OHAM). Comparison of results has been made with the numerical solutions from the literature, and a very good agreement has been observed. Subsequently, effects of governing parameters of the velocity, temperature and concentration profiles are presented graphically and discussed.

Keywords: OHAM; Jeffrey fluid; Heat transfer; Electric field; Thermal radiation; Viscous dissipation; Porous Media

MSC 2010 No.: 76A05, 76M45, 35Q35, 35Q79

1. Introduction

The flow of non-Newtonian fluid over a stretching sheet has caught researchers' interest in the last few years because of its significant practical applications, mainly in manufacturing and industry processes. Many researchers attracted towards the Jeffrey fluid, which is one type of Non-Newtonian fluid, for its simplicity. These flows are occurring in metal and polymer extrusion, cable coating, drawing of plastic sheets, textiles and paper industries, etc. An Industrial application

includes fibers spinning, hot rolling, continuous casting, and glass blowing. In industrial applications and natural process, a number of transportation processes occur where the transfer of heat and mass takes place at the same time as a result of diffusion of chemical species and thermal diffusion.

Sakadis (1961) introduced the study of the boundary layer flow over a stretching surface and formulated boundary layer equations. Crane (1970) examined the boundary layer flow and heat transfer over the stretching plate. The problem considered by Crane was further extended and developed to heat and mass transfer with the effect of blowing or suction by Gupta and Gupta (1977). The problem of boundary layer flow of a viscous fluid by a stretching sheet was studied by Ariel (2009). A few numbers of research papers deal with on the characteristics of Newtonian fluid flow are accessible in the open literature which can be found in (Dessie and Kishan (2014); Ishak et al. (2009); Madaki et al. (2017); Pal (2009); Zheng et al. (2013)).

All the above-mentioned researchers are limited to Newtonian fluid flows. Non-Newtonian fluids are fluids which do not follow Newton's law of motion. Many researchers studied the characteristics of Jeffrey fluid (Non-Newtonian fluid) in different conditions because of its versatile in nature (Akram & Nadeem (2013); Hayat et al. (2011); Hayat et al. (2016); Malik et al. (2012); Nadeem et al. (2010); Qasim (2013); Sahoo (2010); Sandeep et al. (2016)). The resistance force produced by the internal friction between the pore structure (in the porous medium) and fluid is characterized by Darcy's semi-empirical law established by Darcy, see Bear (1972).

In the literature, the following analytical methods are accessible for the solution of nonlinear problems. Most of the methods like Adomian Decomposition Method (ADM) Huda and Abdelhalim (2018), Variational Iteration Method (VIM)(Xu and Eric, 2013), Differential Transform Method (DTM)(Usman et al. 2017), Radial basis function (Ganji, 2006), Homotopy Perturbation Method (HPM)(Jhankal, 2014), Laplace Transform Method (LTM)(Maqbool et al. 2017), Fourier Transform Method (FTM) Maqbool et al. (2016), Fractional Homotopy Analysis Transform Method (FHATM)(Arshad et al. 2017), are used for solution of weakly nonlinear coupled problems. However, only some methods are used for strongly nonlinear coupled problems.

Researchers studied the perturbation methods to obtain the solution of strongly nonlinear simultaneous problems. These methods collect and group small parameters which cannot be found easily. The methods like Artificial Parameters Method(Liu, 1997), Homotopy Analysis Method (HAM) (Hayat et al. 2015) and Homotopy Perturbation Method (HPM)(He, 1999) were introduced for the small parameter. The above analytic methods joined the homotopy with the perturbation techniques.

OHAM is a semi-analytical technique that is directed forward to apply on different type of problems and the existence of any small or large parameters are not significant. Marinca et al. (2009) were initially introduced the basic concept of this method in 2008. OHAM reduces the extent of the computational domain. It is a reliable analytical technique and has already been successfully applied to various nonlinear coupled differential equations occurring in science, engineering and other fields of studies. Many researchers applied OHAM to study the fluid flow problems (Abdel-Wahed et al. (2015); Mabood et al. (2013); Gossaye and Kishan (2018); Mustafa (2016); Ullah et al. (2015)).

Jeffrey fluid is a kind of non-Newtonian fluid that uses a relatively simpler linear model using time derivatives, which are used by many fluid models. Lately, this model fluid has motivated researchers for active discussion on it. Many studies on this fact can be found in (Ahmad and Ishak (2017); Eldabe et al. (2018); Kirani et al. (2017); Odelu et al. (2017); Selvi et al. (2017)). In view of the above discussion, the aim of this paper is to survey the effects of thermal radiation and chemical reaction on electrical MHD Jeffrey fluid flow surrounded in a porous medium over a stretching surface with a heat source and viscous dissipation using OHAM.

2. Basic Concept of Optimal Homotopy Asymptotic Method (OHAM)

Let us apply the analytic method OHAM to the following differential equation (Marinca and Herisanu (2015))

$$L(u(\eta)) + N(u(\eta)) + g(\eta) = 0, \quad B(u) = 0, \quad (1)$$

where L is a linear operator, η represents the independent variable, $u(\eta)$ is an unknown function (a function to be obtained), $g(\eta)$ is a known function, N is a nonlinear operator and B is a boundary operator. First, we have to build a family of an equation using OHAM:

$$[L(\phi(\eta, p)) + g(\eta)](1 - p) - H(p)[L(\phi(\eta, p)) + g(\eta) + N(\phi(\eta, p))] = 0, \quad B(\phi(\eta, p)) = 0, \quad (2)$$

where $p \in [0, 1]$ is an embedding parameter, $H(p)$ is a nonzero auxiliary function ($H(p) \neq 0$) for $p \neq 0$ and $H(p) = 0$ for $p = 0$, $\phi(\eta, p)$ is an unknown function. Clearly, when $p = 0$ and $p = 1$, it holds that:

$$\phi(\eta, 0) = u_0(\eta), \quad \phi(\eta, 1) = u(\eta). \quad (3)$$

Thus, as p increases from 0 to 1, the solution $\phi(\eta, p)$ changes from $u_0(\eta)$ to the solution $u(\eta)$, where $u_0(\eta)$ is obtained from Equation (2) for $p = 0$:

$$L(u_0(\eta)) + g(\eta) = 0, \quad B(u_0) = 0. \quad (4)$$

We choose auxiliary function $H(p)$ in the form

$$H(p) = pC_1 + p^2C_2, \quad (5)$$

where C_1 and C_2 are constants (convergence parameters) which can be determined later. Expanding $\phi(\eta, p)$ in a series form with respect to p , we have

$$\phi(\eta, p, C_i) = u_0(\eta) + \sum_{k \geq 1} u_k(\eta, C_i) p^k, \quad i = 1, 2. \quad (6)$$

Now substituting Equation (6) into Equation (2) and equating the coefficients of like powers of p , and equating each coefficient of p equal to zero, we obtain set of the differential equation with boundary conditions. In general, the solution of Equation (1) can be obtained approximately in the form of

$$\tilde{u}^{(m)} = u_0(\eta) + \sum_{k=1}^m u_k(\eta, C_i). \quad (7)$$

Substituting Equation (7) into Equation (1), we obtain the residual given below

$$R(\eta, C_i) = L\left(\tilde{u}^{(m)}(\eta, C_i)\right) + N\left(\tilde{u}^{(m)}(\eta, C_i)\right) + g(\eta). \quad (8)$$

If $R(\eta, C_i) = 0$, then $\tilde{u}^{(m)}(\eta, C_i)$ is much closer to the exact solution. To reduce the occurred error for nonlinear problems, we have the following relation

$$J(C_1, C_2) = \int_c^d R^2(\eta, C_1, C_2) d\eta, \quad (9)$$

where c and d are the constant values which are depended on the given nonlinear problem. The unknown constants (convergence of parameters) $C_i (i = 1, 2)$ can be obtained from the conditions:

$$\frac{\partial J}{\partial C_1} = \frac{\partial J}{\partial C_2} = 0. \quad (10)$$

With these known convergence parameters, the solution of Equation (7) will be determined.

3. Formulation of the Problem

Let us consider the constitutive equations for a steady, incompressible Jeffrey fluid flow which is given by (Sharma et al. 2017)

$$\tau = -pI + S, \quad (11)$$

$$S = \frac{\mu}{1 + \lambda} \left[R_1 + R_1 \lambda_1 \left(\frac{\partial R_1}{\partial t} + V \cdot \nabla \right) \right], \quad (12)$$

where τ is the Cauchy stress tensor, S is the extra stress tensor, p is the pressure, I represents a unit tensor, μ is the dynamic viscosity, λ is the ratio of relaxation to retardation times, λ_1 is the retardation time of the fluid and R_1 is the Rivlin-Ericksen tensor defined by $R_1 = \nabla V + (\nabla V)^t$.

The steady two-dimensional incompressible flow of an electrically conducting Jeffrey fluid over a stretching surface in the presence of electric field and thermal radiation has been considered. The effect of surface temperature and viscous dissipation has been also considered in the study. The stretching of the surface from a slot through two equal and opposite forces causes the Jeffrey fluid flow. Magnetic field B_0 and electric field E_0 are both applied normal to the Jeffrey fluid flow field.

The sheet xz – plane is stretched in the x -direction, such that the velocity components in the x -direction changes linearly along it (Figure 1).

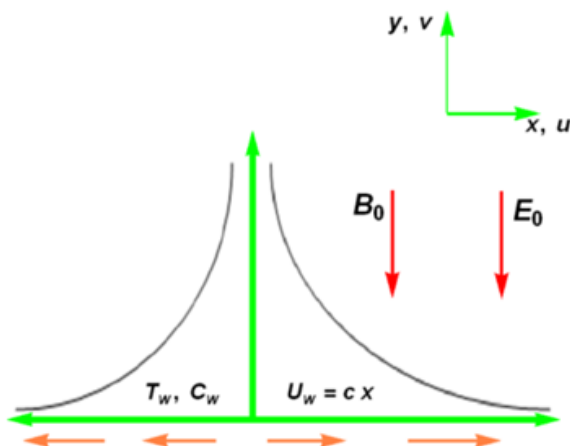


Figure 1. Physical model and co-ordinate system

The two-dimensional electrical MHD boundary layer flow equations of an incompressible Jeffrey fluid are given as:

$$\frac{\partial u}{\partial x} + \frac{\partial v}{\partial y} = 0, \tag{13}$$

$$\frac{v}{1 + \lambda} \left(\frac{\partial^2 u}{\partial y^2} + \lambda_1 \left(u \frac{\partial^3 u}{\partial y^2 \partial x} + v \frac{\partial^3 u}{\partial y^3} + \frac{\partial u}{\partial y} \frac{\partial^2 u}{\partial x \partial y} - \frac{\partial u}{\partial x} \frac{\partial^2 u}{\partial y^2} \right) \right) - \left(\frac{\sigma B_0^2}{\rho} u + \frac{v}{K'_p} u \right) + \frac{\sigma}{\rho} B_0 E_0 = u \frac{\partial u}{\partial x} + v \frac{\partial u}{\partial y}, \tag{14}$$

$$u \frac{\partial T}{\partial x} + v \frac{\partial T}{\partial y} = \alpha \frac{\partial^2 T}{\partial y^2} + \frac{Q_0(x)}{\rho C_p} (T - T_\infty) - \frac{1}{\rho C_p} \frac{\partial q_r}{\partial y} + \frac{\mu}{\rho C_p} \left(\frac{\partial u}{\partial y} \right)^2 + \frac{\sigma}{\rho C_p} (u B_0 - E_0)^2, \tag{15}$$

$$u \frac{\partial C}{\partial x} + v \frac{\partial C}{\partial y} = D \frac{\partial^2 C}{\partial y^2} - k_c^* (C - C_\infty), \tag{16}$$

where u and v are the velocity components in the x – axis and y – axis respectively, T is the fluid temperature, C is the concentration, ν is the kinematic viscosity, ρ is the fluid density, C_p is specific heat and D is the diffusion coefficient. We also have $B_0, E_0, K'_p, k_c^*, \alpha, q_r, Q_0$ and σ which represents the magnetic field factor, electric field factor, the permeability of the porous medium, the rate of chemical reaction, thermal diffusivity, radiative heat flux, heat source coefficient, and electrical conductivity.

Rosseland's approximation for thermal radiation gives $q_r = -\frac{4\sigma^*}{3k^*} \frac{\partial T^4}{\partial y}$, where σ^* and k^* are the Stefan-Boltzmann constant and the mean absorption number, respectively. It is supposed that the temperature variation within the flow is such that T^4 may be expressed in Taylor series. Expanding T^4 about T_∞ and avoiding the higher order terms, we obtain

$$T^4 = -3T_\infty^4 + 4T_\infty^3 T \quad (17)$$

and

$$\frac{\partial q_r}{\partial y} = -\frac{16\sigma^* T_\infty^3}{3k^*} \frac{\partial^2 T}{\partial y^2}. \quad (18)$$

Substituting Equation (18) to Equation (15), we get

$$\begin{aligned} u \frac{\partial T}{\partial x} + v \frac{\partial T}{\partial y} &= \alpha \frac{\partial^2 T}{\partial y^2} + \frac{Q_0}{\rho C_p} (T - T_\infty) + \frac{16\sigma^* T_\infty^3}{3\rho C_p k^*} \frac{\partial^2 T}{\partial y^2} \\ &+ \frac{\mu}{\rho C_p} \left(\frac{\partial u}{\partial y} \right)^2 + \frac{\sigma}{\rho C_p} (uB_0 - E_0)^2, \end{aligned} \quad (19)$$

subjected to the boundary conditions given below

$$\begin{aligned} u = U_w = cx, v = 0, T = T_w = T_\infty + A_1 \left(\frac{x}{l} \right)^r, \\ C = C_w = C_\infty + A_2 \left(\frac{x}{l} \right)^r \text{ for } y = 0, \end{aligned} \quad (20)$$

$$u \rightarrow 0, \quad T \rightarrow T_\infty, \quad C \rightarrow C_\infty \text{ as } y \rightarrow \infty, \quad (21)$$

in which A_1 and A_2 are constants depending on the properties of the fluid, l is the characteristic length, r is the surface temperature parameter, T_w , C_w , T_∞ , and C_∞ are temperature and species concentration at the wall and far away from the wall respectively.

To convert the governing PDEs into a set of similarity ODEs, we established the following dimensionless parameters:

$$\begin{cases} \eta = \sqrt{\frac{c}{v}} y, & u = cx f'(\eta), & v = -\sqrt{vc} f(\eta), \\ g(\eta) = \frac{T - T_\infty}{T_w - T_\infty}, & h(\eta) = \frac{C - C_\infty}{C_w - C_\infty}. \end{cases} \quad (22)$$

After a long simplification, the transformed momentum, energy and concentration Equations (14), (16) and (19) along with the boundary conditions (20) and (21) are given by

$$f''' - \beta f f'''' + \beta (f'')^2 + (1 + \lambda)(f f'' - (f')^2) - (M + K_2)f' + M E_1 = 0, \tag{23}$$

$$\left(1 + \frac{4}{3} R d\right) g'' + Pr [f g' + Ec (f'')^2 + Q g - r f' g + M Ec (f' - E_1)^2] = 0, \tag{24}$$

$$h'' + Sc (f h' - r f' h - \gamma h) = 0, \tag{25}$$

subject to the boundary conditions

$$\begin{cases} f(0) = 0, & f'(0) = 1, & g(0) = 1, & h(0) = 1, \\ f'(\infty) \rightarrow 0, & f''(\infty) \rightarrow 0, & g(\infty) \rightarrow 0, & h(\infty) \rightarrow 0, \end{cases} \tag{26}$$

where the prime denotes differentiation with respect to η and the other parameters appearing in Equations (23)-(25) are defined as follows:

f' is the dimensionless velocity, g is temperature and h is the concentration, $K_2 = \frac{\nu}{c K_p'}$ is the porosity parameter, $M = \frac{\sigma B_0^2}{c \rho}$ is the magnetic field parameter, $E_1 = \frac{E_0}{U_w B_0}$ is the electric field parameter, $\beta = \lambda_1 c$ is the Deborah number, $Ec = \frac{U_w^2}{A_1 c_p} \left(\frac{l}{x}\right)^r$ is the Eckert number, $Pr = \frac{\nu}{\alpha}$ is the Prandtl number, $Rd = \frac{4\sigma^* T_\infty^3}{k k^*}$ is the thermal radiation parameter, $Q = \frac{Q_0}{c \rho c_p}$ is the heat source parameter, $Sc = \frac{\nu}{D}$ is the Schmidt number, $\gamma = \frac{k_c^*}{c}$ is the chemical reaction parameter, for which when $\gamma > 0$ it leads to destructive chemical reaction while $\gamma < 0$ related to generative chemical reaction, respectively.

4. Analytical Solution Using OHAM

In this section, the OHAM is applied to nonlinear ordinary equations (23)-(25) with the boundary conditions (26) under the following assumption

$$f = f_0 + p f_1 + p^2 f_2, \quad g = g_0 + p g_1 + p^2 g_2, \quad h = h_0 + p h_1 + p^2 h_2, \\ H_1(p) = p C_1 + p^2 C_2, \quad H_2(p) = p C_3 + p^2 C_4, \quad H_3(p) = p C_5 + p^2 C_6,$$

where $p \in [0,1]$ is an embedding parameter, $H_j(p), j = 1,2,3$ is a nonzero auxiliary function, and $C_i, (i = 1,2,3,4,5,6)$ are constants Marinca et al. (2009).

4.1. Analytical Solution of the Momentum Boundary Layer Problems

The OHAM is applied to nonlinear ODE (23) using the assumption below

$$L = f' + f'' \text{ and} \\ N = f''' - \beta f f'''' + \beta (f'')^2 \\ + (1 + \lambda)(f f'' - (f')^2) - (M + K_2)f' + M E_1 - (f' + f''), \tag{27}$$

where L is the linear operator, N is a nonlinear operator. Hence, the OHAM family of equation is given by

$$(1 - p)(f' + f'') = H_1(p)[f''' - \beta f f'''' + \beta (f'')^2 + (1 + \lambda)(f f'' - (f')^2 - (M + K_2)f' + ME_1)]. \quad (28)$$

After simplification, equating the like powers of p – terms and using the boundary conditions (26), we have the following:

Equating the zero order equation p^0 , we obtain

$$f_0' + f_0'' = 0 \quad f_0(0) = 0, \quad f_0'(0) = 1. \quad (29)$$

Equating the first order equation p^1 , we obtain

$$f_1' + f_1'' = f_0'' + f_0' + C_1 \left[\begin{array}{l} f_0''' + (1 + \lambda)(f_0 f_0'' - f_0'^2 - M f_0') \\ -K_2 f_0' + ME_1 - \beta [f_0 f_0'''' - (f_0'')^2] \end{array} \right], \quad (30)$$

$$f_1(0) = 0, \quad f_1'(0) = 0.$$

Equating the second order equation p^2 , we obtain

$$f_2' + f_2'' = C_1 \left[\begin{array}{l} f_1''' + (1 + \lambda)(f_0 f_1'' + f_1 f_0'' - 2f_0' f_1' - f_1'(M + K_2)) \\ ME_1 - \beta [f_1 f_0'''' + f_0 f_1'''' - 2f_0' f_1''] \end{array} \right] + C_2 \left[\begin{array}{l} f_0''' + (1 + \lambda)(f_0 f_0'' - f_0'^2 - (M + K_2)f_0') \\ + ME_1 - \beta [f_0 f_0'''' - (f_0'')^2] \end{array} \right] + f_1' + f_1'', \quad (31)$$

$$f_2(0) = 0, \quad f_2'(0) = 0.$$

After solving the ODEs (29)-(31) with the corresponding boundary conditions, we obtain

$$f_0 = e^{-\eta}(e^\eta - 1), \quad (32)$$

$$f_1 = -C_1 e^{-\eta}(-K_2 + e^\eta K_2 - M + e^\eta M - E_1 M + e^\eta E_1 M - K_2 \eta - M \eta + \beta - e^\eta \beta + \eta \beta - \lambda + e^\eta \lambda - K_2 \lambda + e^\eta K_2 \lambda - M \lambda + e^\eta M \lambda - E_1 M \lambda + e^\eta E_1 M \lambda - \eta \lambda - K_2 \eta \lambda - M \eta \lambda - e^\eta E_1 M \eta \lambda) - e^\eta E_1 M \eta. \quad (33)$$

The other term f_2 is too large to mention here. Hence, the solution $f(\eta, C_i)$ is given by:

$$f(\eta, C_i) = f_0(\eta) + f_1(\eta, C_i) + f_2(\eta, C_i). \quad (34)$$

The residual equation for the above problem is written in the form

$$R_1(\eta, C_i) = \left[\begin{array}{l} f''' - \beta f f'''' + \beta (f'')^2 + ME_1 \\ + (1 + \lambda)(f f'' - (f')^2 - f'(M + K_2)) \end{array} \right]. \tag{35}$$

The unknown convergence parameters C_1 and C_2 can be optimally identified from the following conditions given below

$$\frac{\partial J_1(C_1, C_2)}{\partial C_1} = \frac{\partial J_1(C_1, C_2)}{\partial C_2} = 0, \quad \text{where } J_1(C_i) = \int_0^5 R_1^2(\eta, C_i) d\eta. \tag{36}$$

In the particular case when $K_2 = \beta = 0.2, M = E_1 = 0.1$ and $\lambda = 2$, the convergence parameters are as follows

$$C_1 = 0.261227 \text{ and } C_2 = 0.0000449066.$$

Hence, the approximate analytical solution can be written as

$$f(\eta, C_i) = e^{-\eta}(e^\eta - 1) + f_2(\eta, C_i) - 0.261227e^{-\eta} \begin{pmatrix} -0.31 + 0.2e^\eta + 0.1e^\eta + 0.01e^\eta - 0.1\eta \\ -0.2 - 0.2e^\eta - 2.82 + 2e^\eta + 0.4e^\eta + 0.2e^\eta \\ +0.02e^\eta - 2.2\eta - 0.4\eta - 0.02e^\eta\eta - 0.01e^\eta\eta \end{pmatrix}. \tag{37}$$

After substituting all the parameters, the solution is given by

$$f(\eta) = e^{-\eta}(-1 + e^\eta) - 0.261227e^{-\eta}(-2.73 + 2.73e^\eta - 2.7\eta - 0.03e^\eta\eta) + \frac{1}{2}e^{-\eta}(-0.815533897648 + 0.8155339786e^\eta - 0.823430904 + 0.00789700620598e^\eta\eta - 0.49173416508141\eta^2). \tag{38}$$

4.2. Analytical Solution of the Thermal Boundary Layer Problems

The OHAM is applied to nonlinear ODE (24) using the following assumption

$$L = g' + g \text{ and}$$

$$N = \left(1 + \frac{4}{3}Rd\right)g'' + Pr \left[\begin{array}{l} fg' + Ec(f'')^2 + Qg \\ -rf'g + MEc(f' - E_1)^2 \end{array} \right] - (g' + g), \tag{39}$$

where L is the linear operator, N is a nonlinear operator. Hence, the OHAM family of equation is given by

$$(1 - p)(g' + g) = H_2(p)\left[\left(1 + \frac{4}{3}Rd\right)g'' + Pr[f_0g' + Ec(f_0'')^2 + Qg - rf_0'g + MEc(f_0' - E_1)^2]\right]. \quad (40)$$

After simplification, equating the like powers of p – terms and using the boundary conditions (26), we have the following:

Equating the zero order equation p^0 , we get

$$g_0' + g_0 = 0, \quad g_0(0) = 1. \quad (41)$$

Equating the first order equation p^1 , we get

$$g_1' + g_1 = g_0' + g_0 + C_3\left[\left(1 + \frac{4}{3}Rd\right)g_0'' + Pr[f_0g_0' + Ec(f_0'')^2 + Qg_0 - rf_0'g_0 + MEc(f_0' - E_1)^2]\right], \quad (42)$$

$$g_1(0) = 0.$$

Equating the second order equation p^2 , we obtain

$$g_2' + g_2 = g_1' + g_1 + C_3\left[\left(1 + \frac{4}{3}Rd\right)g_1'' + Pr\left[\frac{f_1g_0' + f_0g_1' + 2Ec f_0'' f_1''}{-rf_0'g_1 - rf_1'g_0 + MEc(f_1' - E_1)^2}\right]\right] + C_4\left[\left(1 + \frac{4}{3}Rd\right)g_0'' + Pr\left[\frac{f_0g_0' + Ec(f_0'')^2}{+Qg_0 - rf_0'g_0 + MEc(f_0' - E_1)^2}\right]\right], \quad g_2(0) = 0. \quad (43)$$

After solving the ODEs (41)-(43) with the corresponding boundary conditions, we obtain

$$g_0 = e^{-\eta} \quad (44)$$

$$g_1 = C_3 e^{-2\eta}(-Pr + e^\eta Pr - EcPr + e^\eta EcPr - EcMPr + e^\eta EcMPr - e^\eta(E_1)^2 EcMPr + e^{2\eta}(E_1)^2 EcMPr + r Pr - re^\eta Pr - e^\eta Pr\eta - 2e^\eta E_1 EcMPr\eta + e^\eta PrQ\eta + e^\eta R\eta). \quad (45)$$

The other term g_2 is too large to mention here. Hence, the solution $g(\eta, C_i)$ is given by:

$$g(\eta, C_i) = g_0(\eta) + g_1(\eta, C_i) + g_2(\eta, C_i), i = 1, 2, 3, 4. \quad (46)$$

The residual equation for the above problem is written in the form

$$R_2(\eta, C_i) = \left(1 + \frac{4}{3}Rd\right)g'' + Pr \left[\begin{matrix} fg' + Ec(f'')^2 + Qg \\ -rf'g + MEc(f' - E_1)^2 \end{matrix} \right]. \tag{47}$$

The unknown convergence parameters C_i can be optimally identified from the following conditions given below

$$\frac{\partial J_2(C_i)}{\partial C_1} = \frac{\partial J_2(C_i)}{\partial C_2} = \frac{\partial J_2(C_i)}{\partial C_3} = \frac{\partial J_2(C_i)}{\partial C_4} = 0, \quad \text{where } J_2(C_i) = \int_0^5 R_2^2(\eta, C_i) d\eta. \tag{48}$$

In the particular case when $K_2 = Rd = Ec = Sc = Q = M = E_1 = 0.1, \beta = \gamma = \lambda = 0.2, r = 2$ and $Pr = 0.72$, then the values of the convergence parameters are given by

$$C_1 = 0.6811505642327639, \quad C_2 = 0.602294011253409, \\ C_3 = 0.4671549443900552, \quad C_4 = 0.3843015490314871.$$

Hence, the approximate analytical solution can be written as

$$g(\eta, C_i) = g_2(\eta, C_i) + e^{-\eta} + 0.46715494e^{-2\eta}(Pr(-1 + e^\eta - Ec + e^\eta Ec) \\ - EcMPr + e^\eta EcMPr - e^\eta (E_1)^2 EcMPr + e^{2\eta} (E_1)^2 EcMPr \\ + r Pr - e^\eta Pr(r + \eta) - 2e^\eta E_1 EcMPr\eta + \eta e^\eta (PrQ + R)). \tag{49}$$

After substituting all the parameters, the solution is given by

$$g(\eta) = 0.46715494e^{-2\eta}(0.64079 - 0.64087e^\eta + 0.0007e^{2\eta} + 0.4839e^\eta\eta) \\ + \frac{1}{2}e^{-3\eta}(-5.551115123125 \times 10^{-17} + 0.026877017826e^\eta \\ + 0.00008244963299996e^{3\eta} + 0.0662893612393148e^\eta\eta \\ + 0.2549535423923659e^{2\eta}\eta + 0.04861279751992115e^{2\eta}\eta^2 \\ - 0.02695946745954858e^{2\eta}) + e^{-\eta}. \tag{50}$$

4.3. Analytical Solution of the Concentration Boundary Layer Problems

The OHAM is applied to the nonlinear ODE (25) under the following assumption

$$L = h' + h \text{ and } N = h'' + Sc(fh' - rf'h - \gamma h) - (h' + h), \tag{51}$$

where L is the linear operator, N is a nonlinear operator. Hence, the OHAM family of the equation is given by

$$(1 - p)(h' + h) = H_3(p)[h'' + Sc(fh' - rf'h - \gamma h)]. \tag{52}$$

After simplification, equating the like powers of p – terms and using the boundary conditions (26), we have the following:

Equating the zero order equation p^0 , we get

$$h'_0 + h = 0, \quad h_0(0) = 1. \quad (53)$$

Equating the first order equation p^1 , we get

$$h'_1 + h_1 = h'_0 + h_0 + C_5[h''_0 + Sc(f_0h'_0 - rf'_0h_0 - \gamma h_0)], h_1(0) = 0. \quad (54)$$

Equating the second order equation p^2 , we obtain

$$h'_2 + h_2 = C_5[h''_1 + Sc(f_0h'_1 + f_1h'_0 - rf'_0h_1 - rf'_1h_0 - \gamma h_1)] \\ + C_6[h''_0 + Sc(f_0h'_0 - rf'_0h_0 - \gamma h_0)] + h'_1 + h_1, h_2(0) = 0. \quad (55)$$

After solving the ODEs (53)-(55) with the corresponding boundary conditions, we obtain

$$h_0 = e^{-\eta}, \quad (56)$$

$$h_1 = -C_5e^{-2\eta}(Sc - e^\eta Sc - rSc + e^\eta rSc - e^\eta \eta + e^\eta Sc\eta + e^\eta Sc\eta\gamma). \quad (57)$$

The other term h_2 is too large to mention here. Hence, the solution $h(\eta, C_i)$ is given by:

$$h(\eta, C_i) = h_0(\eta) + h_1(\eta, C_i) + h_2(\eta, C_i), i = 1, 2, 5, 6. \quad (58)$$

The residual equation for the above problem is written in the form

$$R_3(\eta, C_i) = h'' + Sc(fh' - rf'h - \gamma h). \quad (59)$$

The unknown convergence parameters C_i can be optimally identified from the following conditions:

$$\frac{\partial J_3(C_i)}{\partial C_1} = \frac{\partial J_3(C_i)}{\partial C_2} = \frac{\partial J_3(C_i)}{\partial C_5} = \frac{\partial J_3(C_i)}{\partial C_6} = 0, \quad \text{where } J_3(C_i) = \int_0^5 R_3^2(\eta, C_i) d\eta. \quad (60)$$

In the particular case when $Rd = Ec = 0.3, Q = 0.4, M = E_1 = 0.1, \gamma = 0.5, Pr = 6.2$

$\lambda = 2, K_2 = \beta = Sc = 0.2$ and $r = 1$. Thus, the convergence parameters are calculated as

$$C_1 = 0.2612266461651084, \quad C_2 = 0.00007659376670304,$$

$$C_5 = 0.6910524293031602, \quad C_6 = 0.7900961769653166.$$

Hence, the approximate analytical solution can be written as

$$\begin{aligned}
 h(\eta) = & e^{-\eta} - 0.6910524293031602e^{-2\eta}(-0.7e^{\eta}\eta) \\
 & + \frac{1}{2}e^{-3\eta}(0.32867798191848(e^{\eta} - e^{2\eta}) + 0.3965614985e^{2\eta} \\
 & + 0.23291806757185493e^{2\eta}\eta^2). \tag{61}
 \end{aligned}$$

According to Dalir (Dalir, 2014), the exact solution of differential equation (23) when the values of the magnetic field, electric field and porosity parameters M , E_1 and K_2 are zero given by

$$f(\eta) = \frac{1 - e^{-n\eta}}{n}, \quad n = \left(\frac{1 + \lambda}{1 + \beta}\right)^{\frac{1}{2}}. \tag{62}$$

The second derivatives of the equation (54) with its velocity gradient at the surface are given by

$$f''(\eta) = -ne^{-n\eta}, \text{ when } \eta \neq 0 \text{ and } f''(0) = -n, \text{ when } \eta = 0. \tag{63}$$

5. Result and Discussions

The system of Equations (23), (24) and (25), along with the boundary conditions (26), has been solved by the optimal homotopy asymptotic method (OHAM). To verify the validity of our results, we have made a comparison of the skin-friction coefficient $f''(0)$ for different values of the elastic parameter of Jeffrey fluid (the Deborah number β) when $M = E_1 = K_2 = 0$ and $\lambda = 0.2$ with the previously published results and an interesting agreement is observed (See Table 1).

Figures 2, 3 and 4 displayed the influence of electric field Parameter E_1 on the velocity field $f'(\eta)$, temperature profile $g(\eta)$ and concentration profile $h(\eta)$, respectively. An increase in the value of electric field parameter E_1 , the velocity boundary layer increases near the stretching sheet considerably. For a remarkable increase in the value of the electric field, the resistance between fluid particles increases and hence Lorentz force tries to enhance the body forces and it leads to increase in the flow of Jeffrey fluid velocity and momentum boundary layer become thicker. In Figure 3 we have seen that the electric field performs as an accelerating force that increases the fluid temperature and thermal boundary layer thickness. A higher value of an electric field is accompanied with thicker and higher the amount of temperature distribution inside the boundary layer region of the neighborhood of the Jeffrey fluid. From Figure 4 we observed that the fluid concentration decreases for a large amount of an electric field parameter E_1 . The rate of mass transfer at sheet increases because of an increment in the value of the electric field.

Table 1. Comparison values of $f''(0)$ for various values of Deborah number β for the case $M = E_1 = K_2 = 0$ and $\lambda = 0.2$

β	Zokri et al. (2017)	Dalir (2014)	Exact	Present Result	Error
---------	---------------------	--------------	-------	----------------	-------

			Solution	(OHAM)	OH.S – Ex.S
0.0	-1.09544512	-1.09641580	-1.09544512	-1.09539762	0.0000475
0.2	-	-1.00124052	-1.00000000	-1.00000000	0.0000000
0.4	-0.92582010	-0.92724220	-0.92582010	-0.92583743	0.0000173
0.6	-	-0.86755715	-0.86602540	-0.86611893	0.0000935
0.8	-0.81649659	-0.81808091	-0.81649658	-0.81672159	0.0002250
1.0	-	-0.77618697	-0.77459667	-0.77499482	0.0003981
1.2	-0.73854899	-0.74010502	-0.73854895	-0.73915253	0.0006035
1.4	-	-0.70859214	-0.70710678	-0.70794355	0.0008367
1.6	-0.67936634	-0.68074654	-0.67936662	-0.68046252	0.0010959
1.8	-	-0.65589608	-0.65465367	-0.65603602	0.0013823
2.0	-0.63245579	-0.63352833	-0.63245553	-0.63415120	0.0016956

Figures 5 and 6 exhibited the profiles of the dimensionless velocity $f'(\eta)$ and the temperature distribution $g(\eta)$ for dissimilar values of Deborah number β . From Figure 5 we observed that the boundary layer thickness and the velocity are increasing functions of the Deborah number β . In contrast, opposing event is observed for the temperature profile as seen in Figure 6.

Figures 7, 8 and 9 show the variation of temperature profiles for dissimilar values of heat source parameter Q , Eckert number Ec and thermal radiation parameter Rd , respectively. Figure 7 represents the impact of heat source parameter on dimensionless temperature $g(\eta)$. A gradual increment of the heat source parameter Q increases the thermal boundary layer thickness which finally leads to higher the temperature profile. Figure 8 demonstrates the impact of Eckert number Ec in the case of Jeffrey fluid. It is seen that an increase in Ec , increase the temperature distribution and hence increase the thermal boundary layer thickness. This leads to the decline of the rate of heat transfer from the surface. It is observed that the temperature has been affected by the thermal radiation, which results to increase in both the temperature and the thermal boundary layer thickness when the values of Rd increases, which is demonstrated in Figure 9.

Figures 10, 11 and 12 demonstrate the variation of concentration fields for dissimilar values of Schmidt number Sc , destructive chemical reaction and generative chemical reaction parameters, respectively. Figure 10 exhibits the graph of concentration profiles for various values of Schmidt number Sc . We observe that concentration declines with a rise in Schmidt number Sc . Thus, for higher values of Schmidt number the concentration of chemically reactive species is larger and lower for small values of Sc . Figures 11 and 12 displayed the influence of chemical reaction parameter γ . The concentration profile $h(\eta)$ decreases with an increment of destructive chemical reaction parameter ($\gamma > 0$). However, $h(\eta)$ increases in the case of generative chemical reaction parameter ($\gamma < 0$).

Figure 13 displays the influence of surface temperature parameter r on the temperature field. It is seen that an increase in r the thermal boundary layer thickness decreases. The wall temperature parameter plays a significant role in managing heat transfer. The effects of the porous medium K_2 of the flow velocity and temperature are displayed in Figures 14 and 15, respectively. The cause of greater obstruction to the Jeffrey fluid flow is an increase in the porosity parameter K_2 , which concludes in the decrement of velocity, whereas the contrary event occurs in the temperature profile.

The influence of magnetic field parameter M on velocity profiles without the electric field and with the electric field is depicted in Figures 16 and 17, respectively. Figure 16 illustrates the impact

of the magnetic field parameter on the velocity profile in the absence of an electric field ($E_1 = 0$). The velocity field significantly reduces with an increase in the values of magnetic field parameter M . It is obvious that the magnetic field depends on Lorenz force, which is stronger for a larger magnetic field. Because of the absence of an electric field, the Lorenz force increases the frictional force, which performs as a retarding force that opposes the Jeffrey fluid flow over a stretching sheet. Figure 17 illustrates that in the presence of an electric field ($E_1 \neq 0$), as the magnetic field parameter M increases, the velocity boundary layer decreases. After a distance of around $\eta \cong 2.16576$ away from the wall, it increases over the stretching sheet strongly. This is due to the fact that the electric field which acts as speeding up the body force, accelerate the Jeffrey fluid flow.

6. Conclusions

In this study, we have examined the effects of flow parameters like; Deborah number, electric field, porous medium, radiation, Eckert number, heat source/sink, chemical reaction, Schmidt number and wall temperature on heat and mass transfer characteristics of the stretching sheet in a Jeffrey fluid. The transformed ordinary equations are solved analytically using the optimal homotopy asymptotic method (OHAM). The graphic illustrations of our results from the influence of relevant parameters on velocity, temperature, and concentration profiles are discussed in detailed. Some of the specific conclusions which have been derived from the study can be summarized as follows:

- The optimal homotopy asymptotic method is clear, effective, reliable and efficient.
- Controlling and adjusting the convergence of the series solution using the convergence parameters are very simple.
- The elasticity of the Jeffrey fluid decreases the temperature closer to the bounding surface.
- Velocity and temperature increase with an increase in an electric field while concentration decreases.
- For higher values of thermal radiation and viscous dissipation, the temperature field shows an increasing behavior.
- Destructive chemical reaction ($\gamma > 0$) and electric field parameters have the tendency to decrease the concentration boundary layer thickness.
- The surface temperature parameter plays a significant role in controlling the heat transfer.

REFERENCES

- Abdel-Wahed, M. S., Elbashbeshy, E. M. A., and Emam, T. G. (2015). Flow and heat transfer over a moving surface with non-linear velocity and variable thickness in a nanofluids in the presence of Brownian motion. *Applied Mathematics and Computation*, 254, 49–62.
- Ahmad, K. and Ishak, A. (2017). MHD Jeffrey fluid flow over a stretching vertical surface in a porous medium. *Propulsion and Power Research*, 6(4), 269–276.
- Akram, S. and Nadeem. (2013). Influence of induced magnetic field and heat transfer on the peristaltic motion of Jeffrey fluid in an asymmetric channel: closed form solutions. *J. Magn. Mater.* 328, 328, 11–20.

- Arshad, S., Siddiqui, A. M., Sohail, A., Maqbool, K., and Zhi Wu, L. (2017). Comparison of optimal homotopy analysis method and fractional homotopy analysis transform method for the dynamical analysis of fractional order optical solitons. *Advances in Mechanical Engineerin*, 9(3), 1–12.
- Sakadis, B.C. (1961). Boundary layer behaviors on continuous solid surface. *AICHE J.*, 7, 221–225.
- Bear, J. (1972). Dynamics of Fluids in Porous Media. *Dover Publications, New York, P.*, 123.
- Crane, J. L. (1970). Flow past a stretching plate. *Zeitschrift Für Angewandte Mathematik Und Physik ZAMP*, 21(4), 645–647. <https://doi.org/10.1007/BF01587695>
- Dalir, N. (2014). Numerical study of entropy generation for forced convection flow and heat transfer of a Jeffrey fluid over a stretching sheet. *Alexandria Engineering Journal*, 53(4), 769–778.
- Dessie, H. and Kishan, N. (2014). MHD effects on heat transfer over stretching sheet embedded in porous medium with variable viscosity, viscous dissipation and heat source/sink,. *Ain Shams Eng Journal* 2014, 5, 967–977.
- Eldabe, N., Shaker, M. O., & Maha, S. A. (2018). Peristaltic Flow of MHD Jeffrey Fluid Through Porous Medium in a Vertical Channel with Heat and Mass Transfer with Radiation. *Journal of Nanofluids*, 7(3), 595–602(8).
- Mabood, F., Khan, W. A., and Ismail, A.I. Md. (2013). Optimal homotopy asymptotic method for flow and heat transfer of a viscoelastic fluid in an axisymmetric channel with a porous wall,. *PLoS ONE*, 8. <https://doi.org/e83581>
- Ganji, D. D. (2006). The application of He's homotopy perturbation method to nonlinear equations arising in heat transfer. *Phys. Lett. A*, 355, 337–341.
- Gossaye, Adem, A. and Kishan, N. (2018). Slip Effects in a Flow and Heat Transfer of a Nanofluid Over a Nonlinearly Stretching Sheet Using Optimal Homotopy Asymptotic Method. *International Journal of Engineering and Manufacturing Science*, 8(1), 25–46.
- Gupta, P. and Gupta, A. (1977). Heat and Mass Transfer on a Stretching Sheet with Suction or Blowing. *Can.J.Chem.Eng.*, 55, 744–746.
- Hayat, T., Awais, M., Asghar, S., and Hendi, A. A. (2011). Analytical solution for the magneto hydrodynamic rotating flow of Jeffrey fluid in a channel. *J. Fluids Eng.*, 133(7). <https://doi.org/10.1115/1.4004300>
- Hayat, T., Qayyum, S., Imtiaz, M., and Alsaedi, A. (2016). Three-dimensional rotating flow of Jeffrey fluid for Cattaneo-Christov heat flux model. *American Institute of Physics*. <https://doi.org/10.1063/1.4942091>
- Hayat, T., Shafiq, A., and Alsaedi, A. (2015). MHD axisymmetric flow of third grade fluid by a stretching cylinder. *Alexandria Engineering Journal*, 54, 205–212.
- He, J. (1999). Homotopy perturbation technique. *Comp. Math. Appl. Mech. Eng.*, 178, 257–262.
- Huda, E., Abdelhalim, O. B., & Ebaid. (2018). The Adomian decomposition method for the slip flow and heat transfer of nanofluid over a stretching sheet. *Romanian Reports in Physics*, 70, 1–16.
- Ishak, A., Jafar, K., Nazar, R., and Pop, I. (2009). MHD stagnation point flow towards a stretching sheet. *Physica A*, 388, 3377–3383.
- Jhankal, A. K. (2014). Homotopy Perturbation Method for MHD Boundary Layer Flow with Low-Pressure Gradient over a Flat Plate. *Journal of Applied Fluid Mechanics*, 7(1), 177–185.
- Kiran, G. R., Upkare, P., and Varsha (2017). Effect of multiple stenoses on flow of a Jeffrey fluid through a porous medium. *International Journal of Pure and Applied Mathematics*, 113(8),

19 – 27.

- Liu, G. L. (1997). New research direction in singular perturbation theory: artificial parameter approach and inverse perturbation technique. *Conf. 7th Mod. Math. Mech.*
- Madaki, A. G., Roslan, R., Kandasamy, R., and Chowdhury, M. S. H. (2017). Flow and heat transfer of nanofluid over a stretching sheet with non-linear velocity in the presence of thermal radiation and chemical reaction. In *AIP Conference Proceedings* (Vol. 1830). <https://doi.org/10.1063/1.4980877>
- Malik, M. ., Zehra, I., and Nadeem, S. (2012). Numerical treatment of Jeffrey fluid with pressure-dependent viscosity. *Int. J. Numer. Meth. Fluids*, 68, 196–209.
- Maqbool, K., Beg, A. O., Sohail, A., and Idreesa, S. (2016). Analytical solutions for wall slip effects on magnetohydrodynamic oscillatory rotating plate and channel flows in porous media using a fractional Burgers viscoelastic model. *THE EUROPEAN PHYSICAL JOURNAL PLUS*. <https://doi.org/10.1140/epjp/i2016-16140-5>
- Maqbool, K., Mann, A. B., and Tiwana, M. H. (2017). Unsteady MHD convective flow of a Jeffrey fluid embedded in a porous medium with ramped wall velocity and temperature. *Alexandria Engineering Journalria Engineering Journal*. <https://doi.org/10.1016/j.aej.2017.02.012>.
- Marinca, V. and Herisanu, N. (2015). *The optimal Homotopy Asymptotic Method*. Springer International Publishing Switzerland. <https://doi.org/10.1007/978-3-319-15374-2>
- Marinca, V., Herisanu, N., Bota, C., and Marica, B. (2009). An optimal homotopy asymptotic method applied to the steady flow of fourth-grade fluid past a porous plate. *Appl Math Lett*, 22, 245–251.
- Mustafa, M. (2016). Viscoelastic flow and heat transfer over a nonlinearly stretching sheet: OHAM solution. *Journal of Applied Fluid Mechanics*, 9, 1321–1328.
- Nadeem, S., Hussain, A., and Khan, M. (2010). Stagnation flow of a Jeffrey fluid over a shrinking sheet. *Z. Nat. A*, 65(6–7), 540–548.
- Odelu, O., Adigoppula, R., and Pravin, K. K. (2017). Influence of thermophoresis and induced magnetic field on chemically reacting mixed convective flow of Jeffrey fluid between porous parallel plates. *Journal of Molecular Liquide*. <https://doi.org/DOI:doi:10.1016/j.molliq.2017.02.061>
- Ariel, P.D. (2009). Extended homotopy perterbation method and computation of flow past a stretching sheet. *Comput. Math. Appl*, 58, 2402–2409.
- Pal, D. (2009). , Heat and mass transfer in stagnation-point flow towards a stretching surface in the presence of buoyancy force and thermal radiation. *Meccanica*, 44, 145–158.
- Qasim, M. (2013). Heat and mass transfer in Jeffrey fluid over a stretching sheet with heat source/sink. *Alexandria Engineering Journal*, 52(4), 571–575.
- Sahoo, B. (2010). Flow and heat transfer of a non-Newtonian fluid past a stretching sheet with partial slip. *Commun.Nonlinear Sci. Numer. Simul*, 15, 602–615.
- Sandeep, N., Sulochana, C., and Isaac Lare, A. (2016). Stagnation-point flow of a Jeffrey nanofluid over a stretching surface with induced magnetic field and chemical reaction. *Int. J. Eng. Res. Africa*, 20, 93–111.
- Selvi, P., Sreenadh, S., Kesava, R. E., and Gopi, K. G. (2017). Viscous Flow of Jeffrey Fluid in an Inclined Channel Through Deformable Porous Media. *World Applied Sciences Journal*, 35(5), 669–677.
- Sharmaa, B. D., Yadava, P. K., and Anatoly, F. (2017). A Jeffrey-Fluid Model of Blood Flow in Tubes with Stenosis. *Colloid Journal*, 79(6), 849–856.

- Ullah, H., Nawaz, R., Islam, S., Idrees, M., and Fiza, M. (2015). The optimal homotopy asymptotic method with application to modified Kawahara equation. *Journal of the Association of Arab Universities for Basic and Applied Science*, 18, 82–88.
- Usman, M., Hamid, M., Khan, U., Mohyud Din, S. T., Iqbal, M. A., and Wang, W. (2017). Differential transform method for unsteady nanofluid flow and heat transfer. *Alexandria Engineering Journal*. <https://doi.org/10.1016/j.aej.2017.03.052>
- Xu, L. and Eric, W. M. L. (2013). Variational Iteration Method for the Magnetohydrodynamic Flow over a Nonlinear Stretching Sheet. *Hindawi Publishing Corporation*. <https://doi.org/10.1155/2013/573782>.
- Zheng, L., Zhang, C., Zhang, X., and Zhang, J. (2013). Flow and radiation heat transfer of a nanofluid over a stretching sheet with velocity slip and temperature jump in porous medium. *Journal of the Franklin Institute*, 350, 990–1007.
- Zokri, S., Arifin, N., Salleh, M., Kasim, A., Mohammad, N., and Yusoff, W. (2017). MHD Jeffrey nanofluid past a stretching sheet with viscous dissipation effect. *Journal of Physics*. <https://doi.org/10.1088/1742-6596/890/1/012002>.

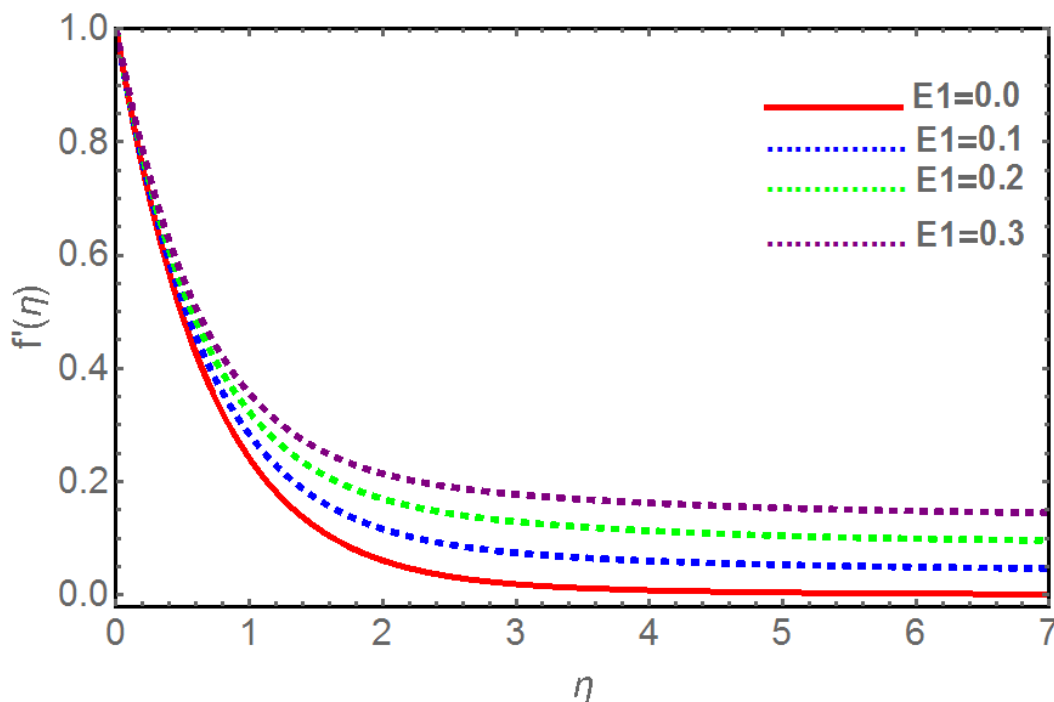


Figure 2. Velocity profile $f'(\eta)$ for different values of electric field parameter E_1 when $K_2 = \beta = 0.5, M = 1, \lambda = 0.2$

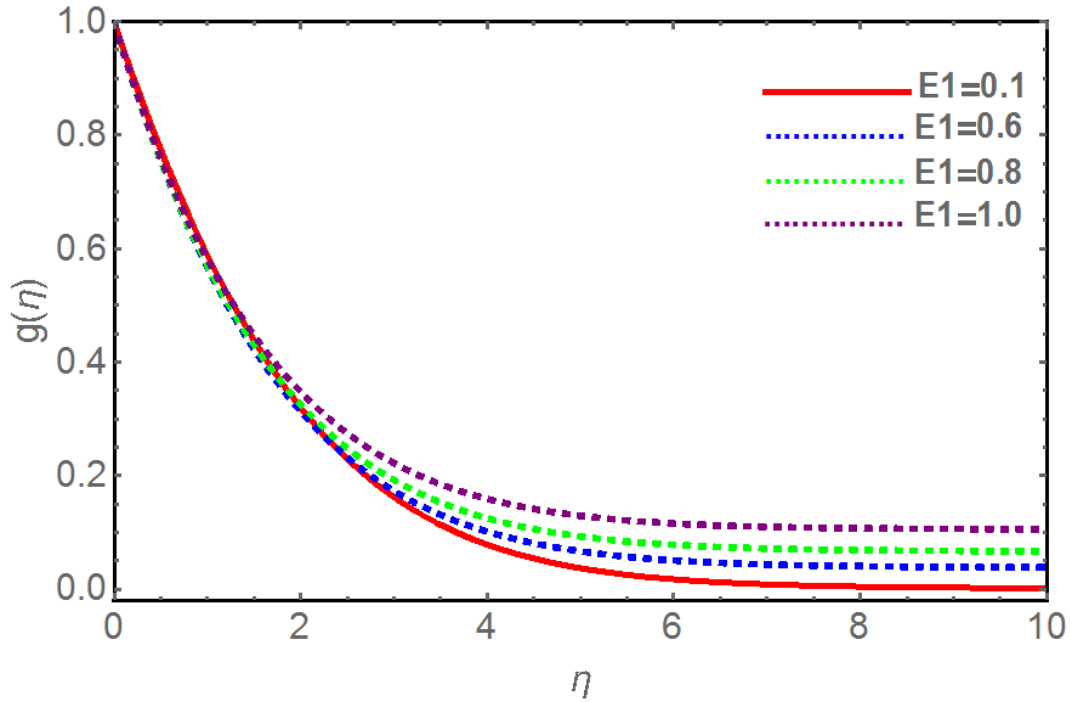


Figure 3. Temperature profile $g(\eta)$ for different values of electric field parameter E_1 when $K_2 = 0.5, Rd = Q = 0.1, M = 0.5, \lambda = \beta = 1, Ec = 0.2, r = 2, Pr = 0.72$

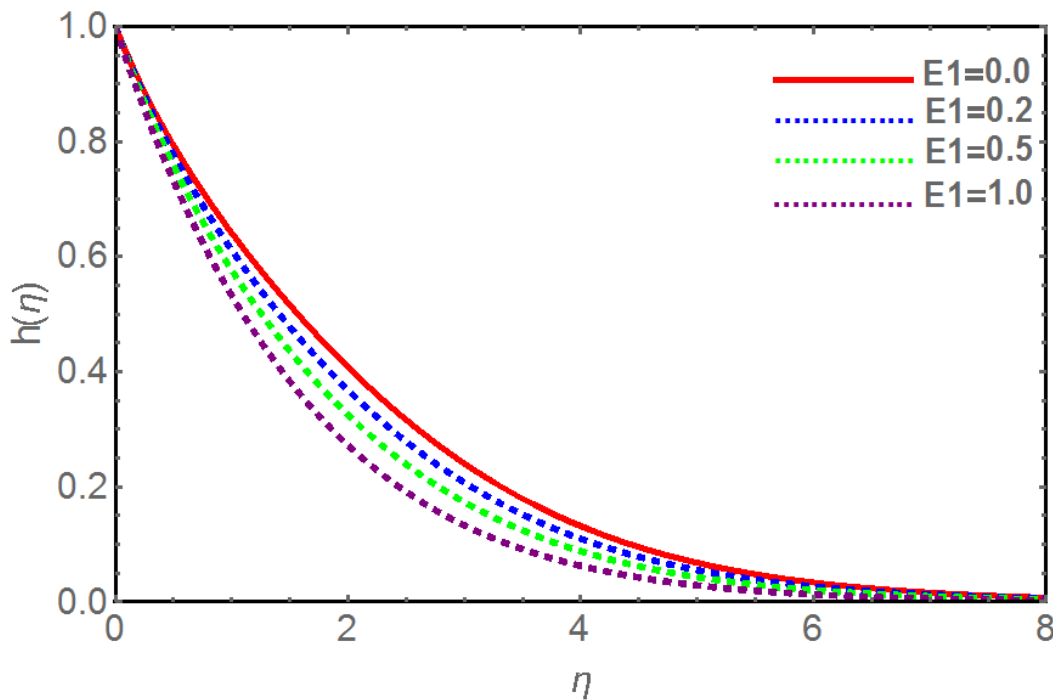


Figure 4. Concentration profile $h(\eta)$ for different values of electric field parameter E_1 when $K_2 = \beta = 0.5, M = 1, \lambda = Sc = \gamma = 0.2, r = 2$

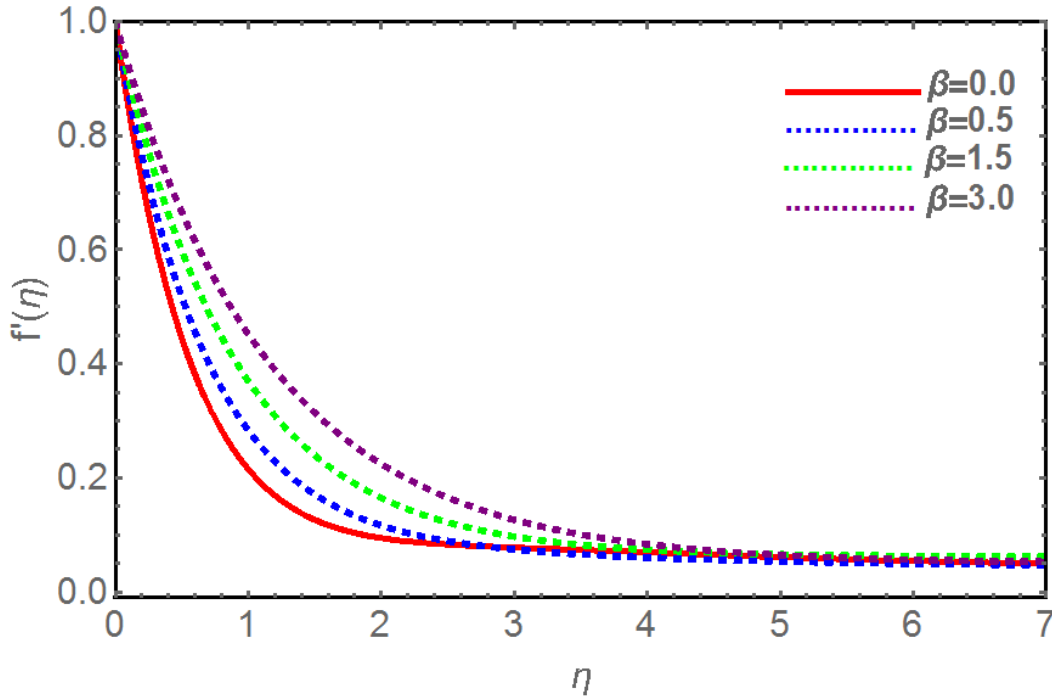


Figure 5. Velocity profile $f'(\eta)$ for different values of β when $K_2 = 0.5, E_1 = \lambda = 0.1, M = 1$

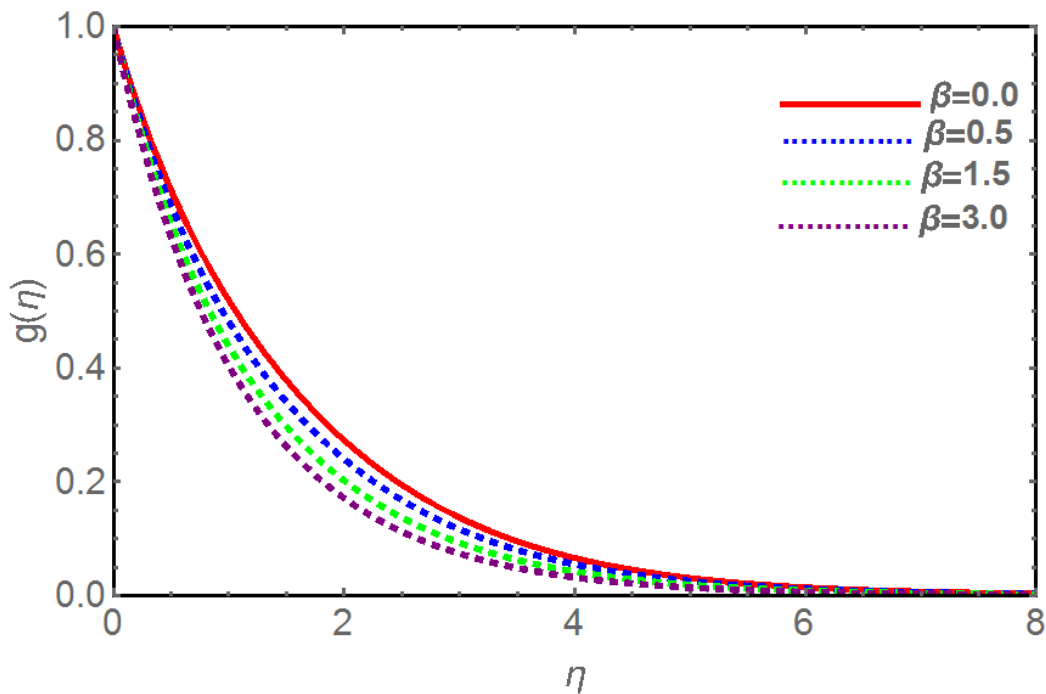


Figure 6. Temperature profile $g(\eta)$ for different values of β when $K_2 = 0.5, E_1 = Rd = Q = 0.1, M = 1, \lambda = Ec = 0.2, r = 2$

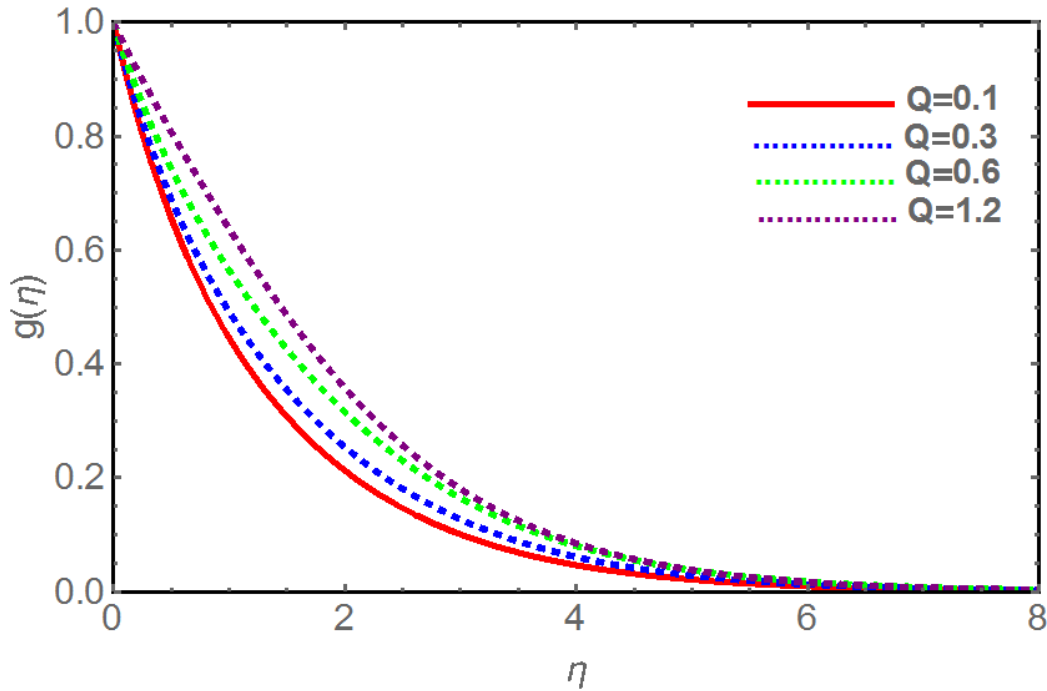


Figure 7. Temperature profile $g(\eta)$ for different values of heat source parameter Q when $K_2 = M = E_1 = Ec = 0.1, r = 2, \lambda = \beta = 0.2, Pr = 0.72$

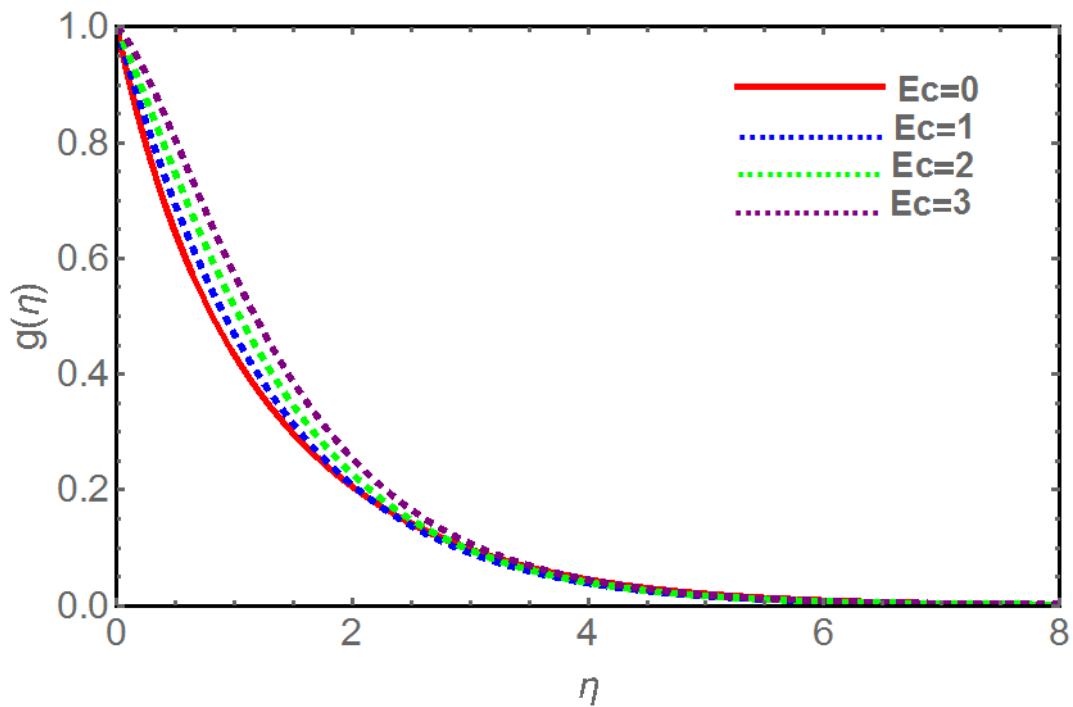


Figure 8. Temperature profile $g(\eta)$ for different values of Eckert number Ec when $K_2 = M = E_1 = Rd = Q = 0.1, \lambda = \beta = 0.2, r = 2, Pr = 0.72$

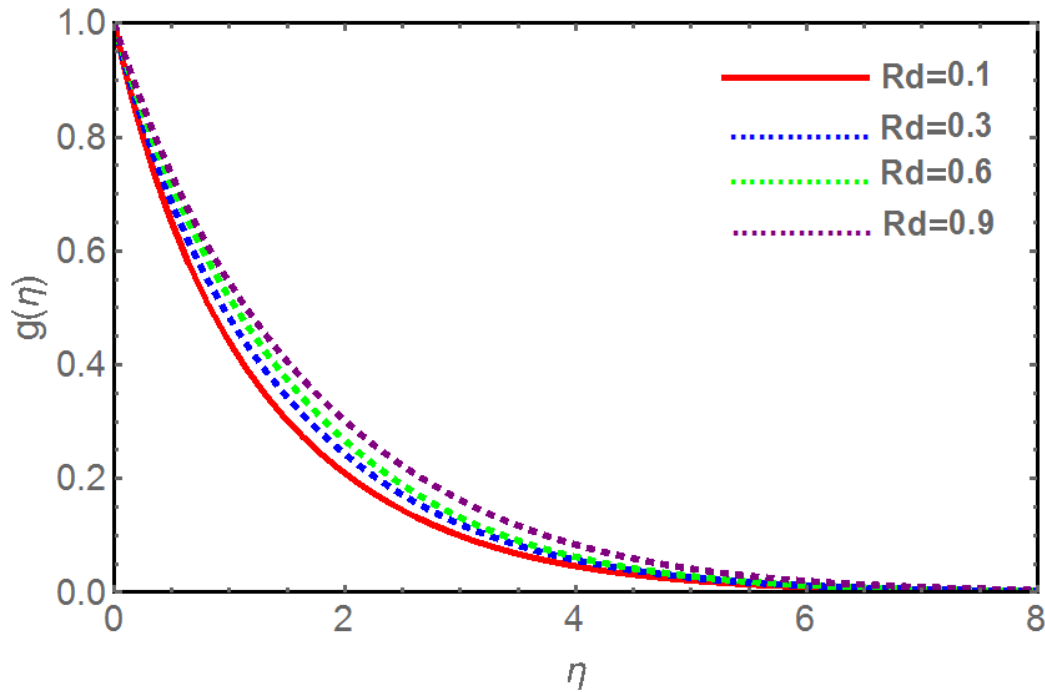


Figure 9. Temperature profile $g(\eta)$ for different values of thermal radiation Rd when $K_2 = M = Q = E_1 = Ec = 0.1, \lambda = \beta = 0.2, Pr = 0.71, r = 2$

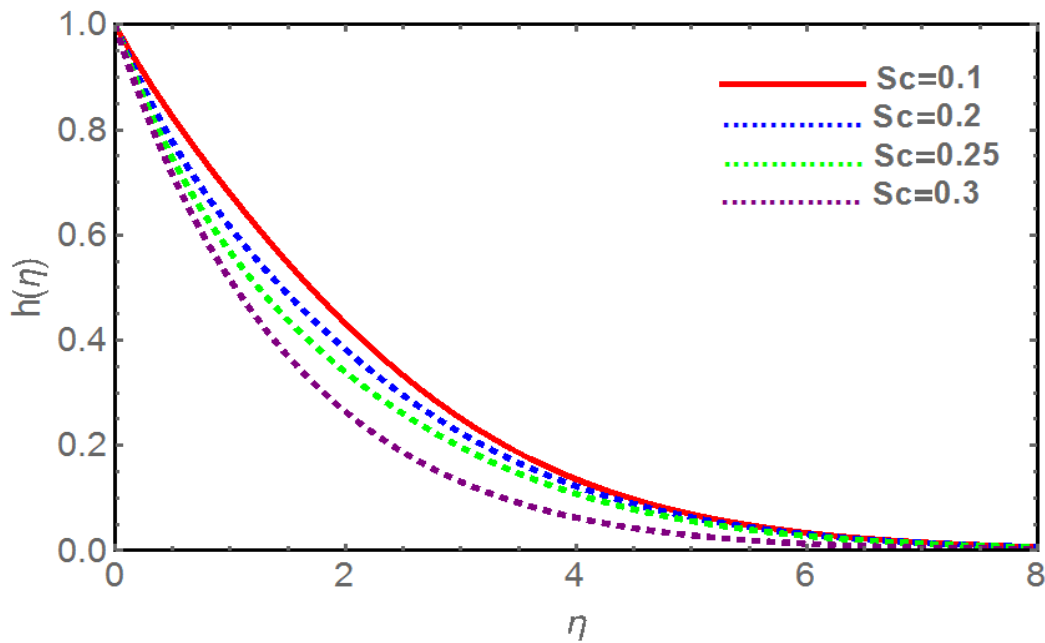


Figure 10. Concentration profile $h(\eta)$ for different values of Schmidt number Sc when $K_2 = M = E_1 = Rd = 0.1, r = 2, \gamma = \lambda = 0.2$

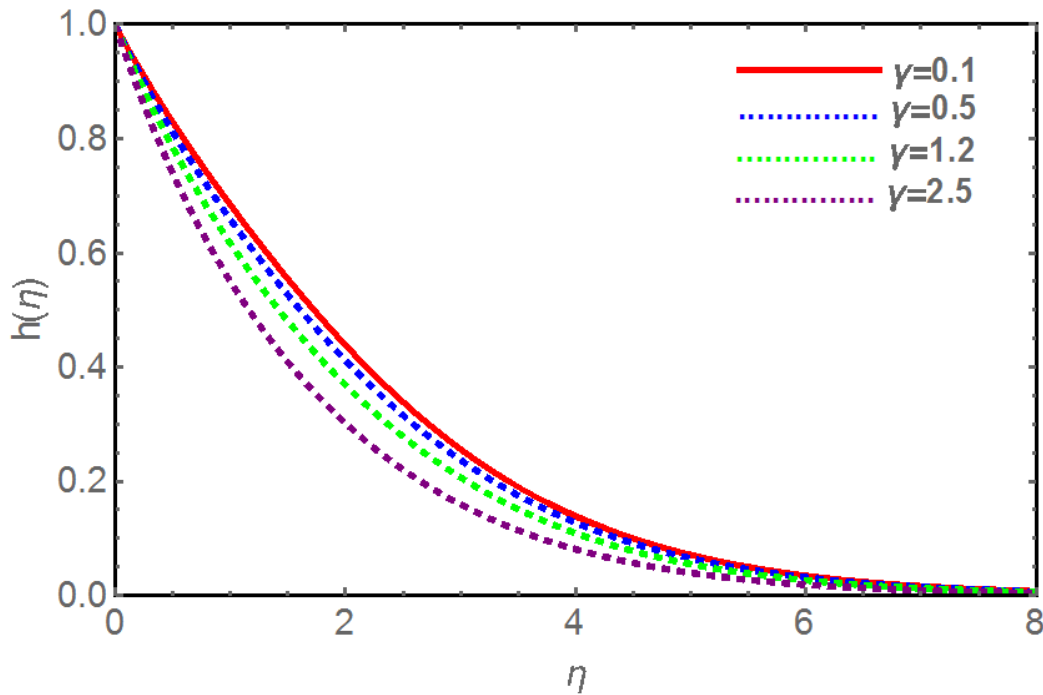


Figure 11. Concentration profile $h(\eta)$ for different values of chemical reaction parameter $\gamma > 0$ when $K_2 = M = E_1 = Rd = Sc = 0.1, r = 2, \lambda = 0.2$

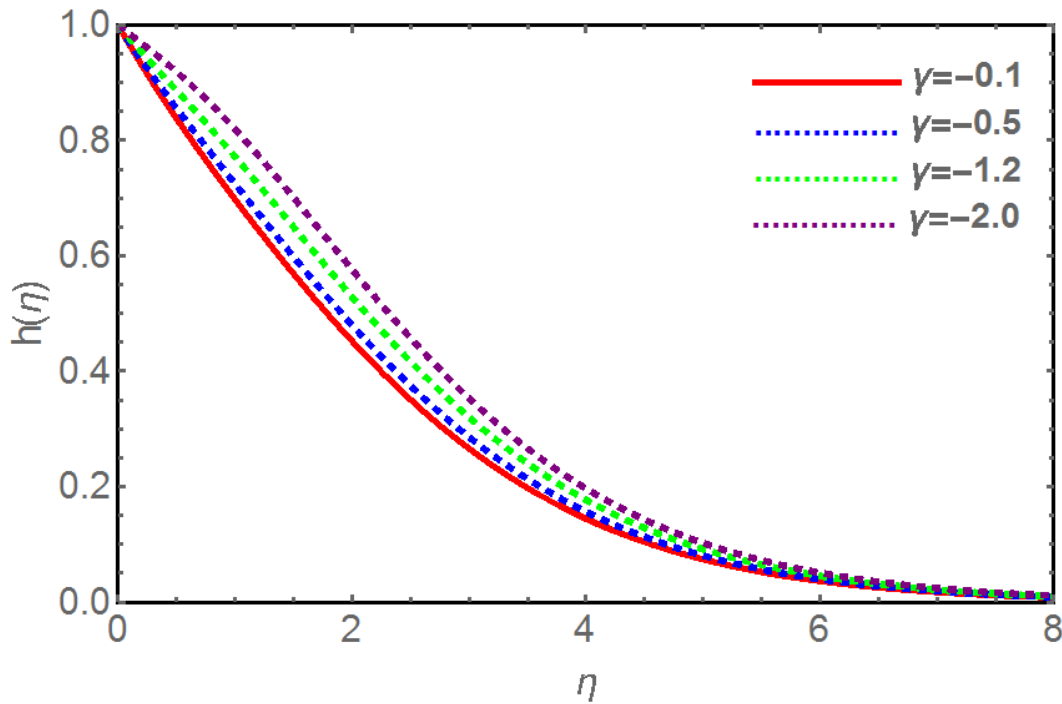


Figure 12. Concentration profile $h(\eta)$ for different values of chemical reaction parameter $\gamma < 0$ when $K_2 = M = E_1 = Rd = Sc = 0.1, r = 2, \lambda = 0.2$

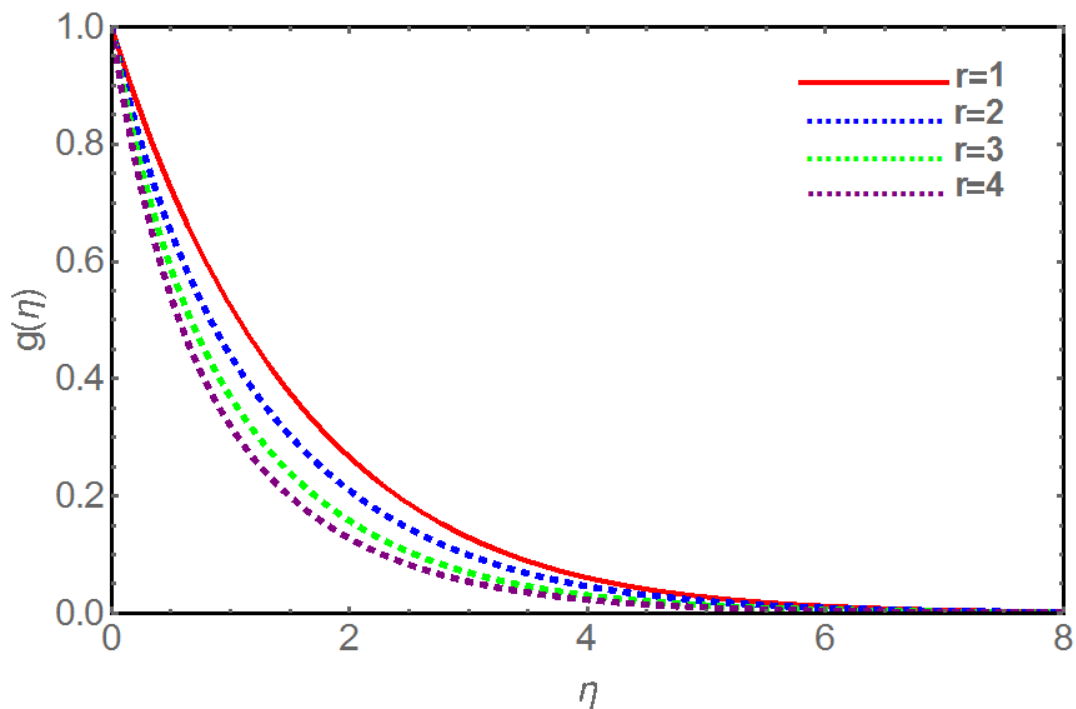


Figure 13. Temperature profile $g(\eta)$ for different values of surface temperature parameter r when $K_2 = M = Q = E_1 = Ec = Rd = 0.1, \lambda = \beta = 0.2, Pr = 0.71$

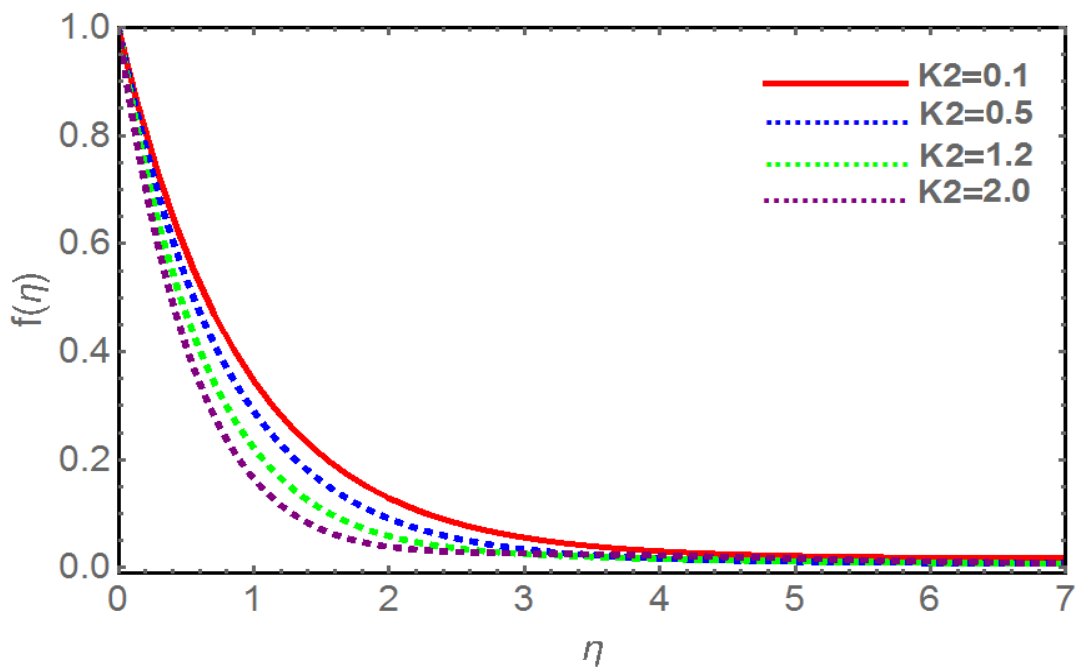


Figure 14. Velocity profile $f'(\eta)$ for different values of porosity parameter k_2 when $\beta = 0.2, E_1 = 0.1, M = 0.1, \lambda = 0.2$

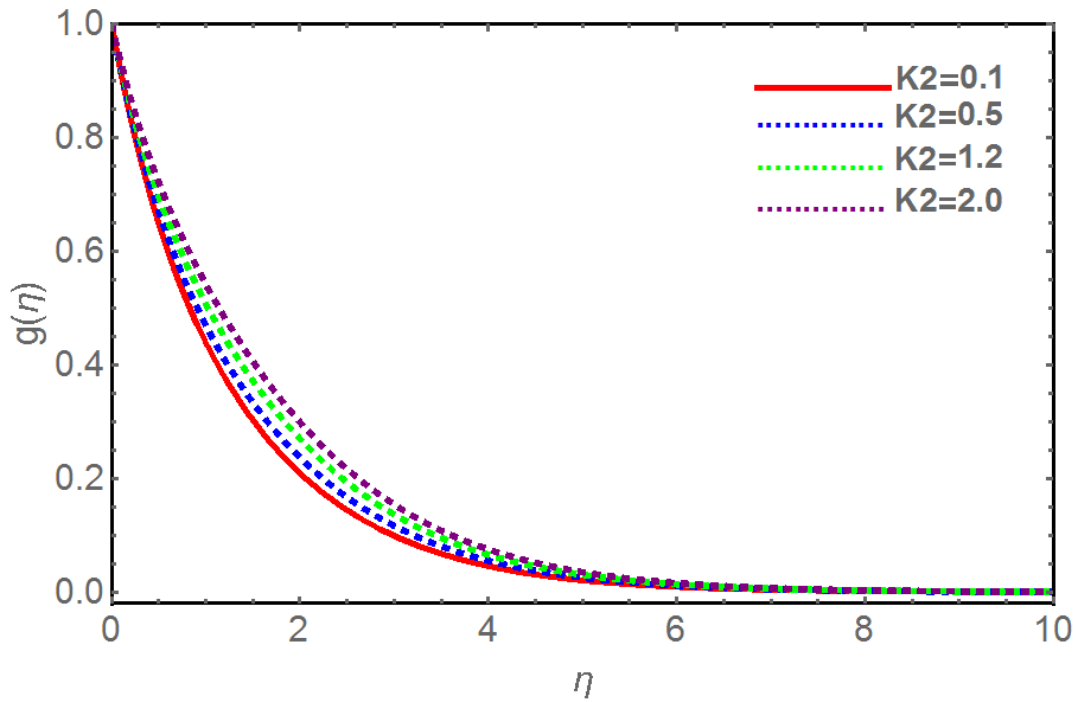


Figure 15. Temperature profile $g(\eta)$ for different values of porosity parameter K_2 when $M = E_1 = Ec = Q = Rd = 0.1, \lambda = \beta = \gamma = 0.2, Pr = 0.71, r = 2$

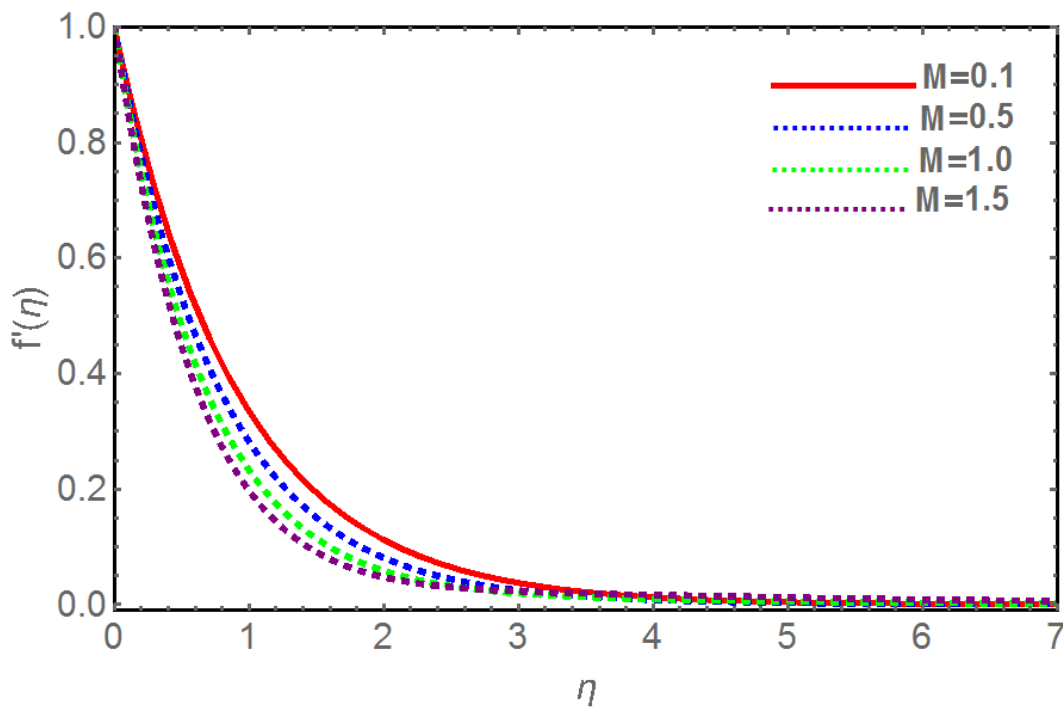


Figure 16. Velocity profile $f'(\eta)$ for different values of magnetic field parameter M with no electric filed ($E_1 = 0$) when $K_2 =, \lambda = \beta = 0.2$

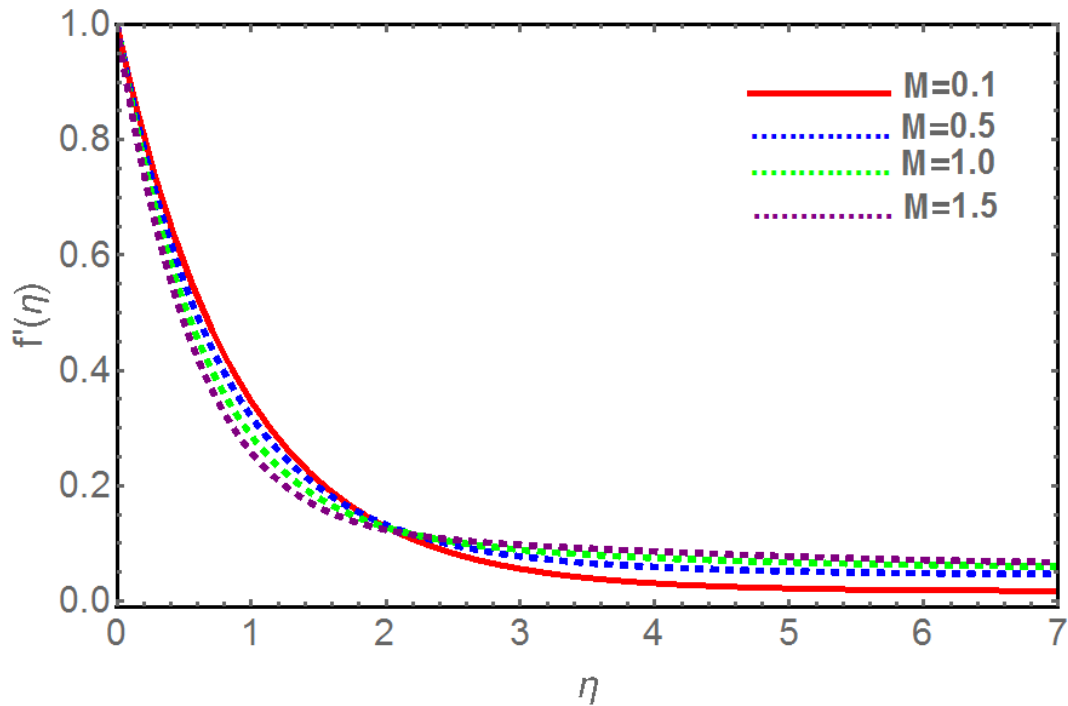


Figure 17. Velocity profile $f'(\eta)$ for different values of magnetic field parameter M when $K_2 = E_1 = 0.1, \lambda = \beta = 0.2$